International Meeting: " Nuclear Power in Eastern Europe: Safety, European Integration, Free Electricity Market"
17-20 June 2001, Varna, Bulgaria

EXTENDED ANALYSIS OF WWER1000 CHARPY TEST DATA

Prof. D.Sc. St.Vodenicharov, Sen. Res. Dr. Tz.Kamenova,
Institute of Metal Science, BAS,67, Shipchenski prohod
1574 Sofia, Bulgaria , E-mail stvims@ims.bas.bg

1. INTRODUCTION

The WWER 1000 RPV steel and weld metal are characterized by lower P - and Cu - and higher Ni content compared to WWER440 RPV steels and welds. In some cases Ni content reaches 1.9%. The influence of Ni content on embrittlement rate of RPV steel is not taken into account in Russian guide calculation formula for ductile to brittle transition temperature prediction [1] and fixed Af values for base and weld metal are proposed. RPV integrity assessment is more reliable when using experimental Tkf value. Impact three - point bending test of surveillance specimens is used according WWER1000 RPV Standard Surveillance Program for determination of temperature dependency of absorbed impact fracture energy (Cv). Cv value could be determined for this purpose by pendulum angle or by integration of area under force - displacement diagram of instrumented Charpy test [2,3]. Analysis of force - displacement diagram permits to gain additional information on the influence of neutron irradiation on crack initiation, propagation and crack arrest [4,5,6].

The aim of this work is to study the embrittlement rate of WWER-1000 RPV weld metal with high Ni content and to determine influence of neutron irradiation on partial energies of ductile crack initiation, stable and unstable crack propagation and post crack arrest.

2. EXPERIMENTAL

Material

Weld metal 10KhGNMFAA (1.70%Ni) was investigated in non-irradiated and irradiated state. The concentration level of impurities P and Cu was 0.009% and 0.05% respectively.

Conditions of irradiation

Standard Charpy V-notched specimens were irradiated in WWER1000 surveillance positions at different neutron fluence (Table 1). The irradiation temperature was not measured experimentally but according [7] it was expected to be in the range 305± 5 ^{o}C.

Mechanical testing

Standard Charpy-V specimens (10x10x55 mm^3) were tested using instrumented ISO 300J pendulum impact testing machine at velocity 5.5m/sec [2,3]. The dependence of absorbed fracture energy on testing temperature was obtained for each material state. The hyperbolic tangent function was used for data fitting.

Ductile to brittle transition temperatures Tkf and shift of Tkf (ΔTkf) were determined at energy levels postulated according Russian standard [1]. It is assumed that the neutron induced shift of Tkf depends on neutron fluence as follows:

$$\Delta Tkf = Tkf - Tko = Af.(F.10^{-18})^{0.333} \qquad (1)$$

where Tko and Tkf are ductile to brittle transition temperatures of as-received metal and irradiated metal respectively, Af - chemical coefficient (depending on chemical composition of the steel), F - neutron fluence.

Impact test load diagram force-displacement was registered for each of specimens. Four partial absorbed fracture energies (LSE, A, B, C) are defined according [4,5,6] (Fig.1a). “LSE” (low shelf energy) includes elastic energy and brittle (lse) crack propagation energy (EΔ). “A” represent ductile initiation energy (energy for onset of ductile crack front from notch across the specimen width), “B”- ductile propagation energy and “C”- post crack arrest energy. The following characteristic temperatures (Fig.1b) could by defined from the temperature dependencies of these four partial energies:

- TI - ductile crack initiation temperature - the temperature corresponding to onset of energy fraction A (A>0)
- T_N - ductility temperature - the temperature corresponding to onset of energy fraction B (B>0). It is supposed that the crack initiation occurs at maximum load.
- To - temperature of Cv impact upper shelf onset i.e. no brittle fracture is initiated (Fu=Fa), onset of fracture C energy to maximum value.

3. RESULTS

3.1. IMPACT TEST RESULTS

The analysis of temperature dependencies of absorbed fracture energy, lateral expansion and shear fracture according [1] showed that the leading criteria for Tkf determination is energy criteria.

The obtained values for ductile to brittle transition temperature shift for each material state are given in Table 1. Mean values of fluence in the transition zone of Charpy curve, ΔTk predicted by Russian standard [1], calculated Af-values and guide Af value are given in the table 1 as well.

Table 1.

Weld metal WM	Fluence (E>0.5MeV) [n/cm^2]	ΔTk [^{o}C]	ΔTkf predicted by Guide [^{o}C]	Af
state 1	4.1E18	21	32	12.5
state 2	5.9.0E18	19	36	10.5
state 3	13.4E18	33	47	14.0
Af mean value				12.3
Af by Guide				20.0

The experimental Af values for these fluence rates are lower than provided by Guide [1]. The obtained ΔTk values are in compliance with the estimated data from low range fluence part of linear ΔTk - fluence dependency given in [8,9]. It should be reminded that the last data have been obtained by testing of specimens, irradiated at neutron flux up to hundred times higher than the service RPV flux.

Prognostic dependence of Tkf shift on fast neutron fluence for the investigated material is demonstrated on Fig.2. The comparison between ΔTkf experimental curve and trend curve calculated according Guide [1] and surveillance trend curves for the other three NPP Units [7,10] shows that the embrittlement rate in our case is lower than the rate expected by Guide, Balakovo 1 and Kalinin 1 data and close to Novovoronezh 5 data.

The observed differences of embrittlement rates of compared weld metals could not be explained by the variations of Ni content only. The variations of P, Cu and other alloying elements concentration, the fluence gradient on specimens, the microstructural unhomogenity and the small number of specimens in the tested series contribute to Af scattering also.

3.2. ANALYSIS OF FORCE-DISPLACEMENT DIAGRAM

Force - displacement diagrams of unirradated and irradiated up to fluence 5.9 and 13.4E18 n/cm2 specimens (state 2 and 3 respectively) were analyzed. The values of characteristic forces Fgy (yield force), Fm (maximal force), Fiu (force at the initiation of unstable crack propagation), Fa (crack arrest force) and values of partial energies A, B and C were determined. Fiu, Fa values for specimens fractured at Cv USE temperature were determined at the point corresponding to deviation of velocity from linearity.

Temperature dependencies of Fgy, Fm, Fiu, Fa for weld metal in unirradiated state and in irradiated states 2 and 3 are presented on Fig.3,4,5. The onset of Cv USE is marked as well. The values of characteristic temperatures determined from cross points of mean curves and presented in Table 2.

Table 2

	CHARACTERISTIC TEMPERATURES DETERMINED BY CHARACTERISTIC F - T CURVES [°C]					
criteria	Fgy=Fm		Fm=Fiu		Fiu=Fa	
	Ti	ΔTi	T_N	ΔT_N	T7	ΔTo
uniradiated	-120	-	-48	-	+18	-
state 2	-80	40	-32	16	+44	26
state 3	-71	49	0	48	+38	20

The scatter of data is too high due to the limited number of tested specimens, the fluence gradient and the microstructural unhomogeneity of weld metal. For this reason no quantitative data analysis but only qualitative conclusions were made. The analysis of temperature dependencies of general yield force for the three material states shows that the Fgy values decrease with fracture temperature. Fgy values are higher for irradiation states. The temperature dependence of maximal force is not well expressed but a slight increase of Fm with neutron irradiation could be predicted. The brittle crack initiation force is decreasing function of test temperature and Fiu/T experimental curves are displaced to higher temperature with the neutron fluence increase. Data show that crack arrest force increases with test temperature and Fa/T curves after neutron irradiation are shifted to higher temperature.

Neutron induced embrittlement of weld metal influences T_I, T_N and To characteristic temperatures. A well expressed shift of ductile crack initiation temperature and ductility temperature to higher temperatures is observed with neutron fluence increase.

Temperature dependencies of A,B,C partial energies are plotted for each metal state using hyperbolic tangent functions (Fig.6,7,8).

T_I and T_N values for weld metal were obtained at 50%USE energy and by approximation of transition zone of A and B curves to y=0. To temperatures were determined by the intersection of transition part and upper shelf part of C curves (onset of Fiu=Fa). The obtained data for the three material states are presented in table 3.

Table 3

CHARACTERISTIC TEMPERATURES DETERMINED BY PARTIAL ABSORBED IMPACT ENERGY [°C]						
energy	A		B		C	
criteria	50% max ------------ A= f(T) slope curve extr.		50% max ------------ B= f(T) slope curve extr.		50% max ------------ C= f(T) slope curve extr.	
	Ti	ΔTi	T_N	Δ T_N	To	ΔTo
unirradiated	-48 ----- -75		-28 ----- -47	-	+8 ----- +54	-
state 2	-36 ----- -58	12 ------ 17	-18 ----- -33	10 ----- 14	+32 ---- +80	24 ---- 26
state 3	-20 -------- -48	28 ----- 27	+4 ---- -13	24 ---- 34	+22 ----- +60	14 ---- 10

The analysis of A,B and C partial fracture energy/temperature curves shows that the slope of ductile crack propagation energy curves is the highest and the slope of post crack arrest energy curves is the lowest one. All curves are shifted by neutron irradiation to higher temperatures. As in the case of the total Cv dependencies the neutron irradiation has no expressed effect on upper shelf values of the three partial energies. A little decrease of USE of partial energies could be supposed but the small number of tested specimens and the microstructure unhomogenity do not permit it's quantitative estimation. It should be noted that the drastic redistribution of A, B and C at different fluence, reported for Yankee Rowe RPV steel [5,6], is not observed for WWER 1000 weld metal. This could be explained by the lower embrittlement capability of WWER 1000 metal and the higher irradiation service temperature.

Some increase of T_I, T_N and To characteristic temperatures, determined by partial energies, is observed after neutron embrittlement. The shifts of characteristic temperatures, 47J shift of critical temperature of embrittlement, 50% shear fracture temperature shift and 0.89mm lateral expansion temperature shift are compared in table 4.

Table 4

TEMPERATURE SHIFT									
Criteria	Partial energy at 50% maximum			Partial energy curve slope extrapolation			47J total energy	50% shear fracture	0.89mm lateral expansion
	ΔT_I	ΔT_N	ΔT_0	ΔT_I	ΔT_N	ΔT_0	ΔTk	$\Delta FATT$	ΔL
state 2	12	10	24	17	14	26	19	9	18
state 3	28	24	14	27	34	10	33	26	30

4. CONCLUSIONS

1. The embrittlement rate of WWER1000 RPV weld metal at fluence up to one quarter end life time fluence of RPV is lower than predicted by Russian standard.
2. The rate of Bulgarian RPV weld metal embrittlement is lower than Balakovo 1 and Kalinin 1 rates.
3. General yield force and maximal force of force-displacement Charpy diagram are higher for irradiated states.
4. Temperature dependencies of all characteristic temperatures after neutron irradiation are shifted to higher temperatures.

5. Ductile crack propagation energy/temperature curve is characterized by a biggest slope and the post crack arrest energy curve - by a smallest slope.
6. A, B, C partial energy/temperature curves are shifted by neutron irradiation to higher temperatures.
7. A faint decrease of maximal values of partial energies A,B and C is observed.
8. Additional irradiation experiments with new surveillance assemblies design which guarantees homogenous neutron field distribution should be performed in order to obtain more reliable parameters of embrittlement process.

REFERENCES

1. Regulatory Document PNAE-G-7-002-86, Strength analysis standarts for equipment and piping at nuclear power plants),1986, Moskow, Energoatomizdat.
2. ISO International standard ISO/14556 (N191)
3. W.Bohme, Experiance with Instrumented Charpy tests obtained by DVM round robin and future developments, Evaluation of Material Properties by Dinamic Fracture, ed. E. van Walle, 1996 MEP, London
4. A.Fabry, E. van Walle, J. van de Velde, R.Chaouadi, J.Puzzolante, Th. Van Ransbeek, , On the use of the instrumented Charpy V impact signal for assessment of RPVS embrittlement, Evaluation of Material Properties by Dynamic Fracture, ed. E. van Walle, 1996 MEP, London,p.59, p.1
5. A.Fabry, E. van Walle, R.Chaouadi, J. Wannijn, A.Verstrepen, J.Puzzolante, Th. Van Ransbeek , J. van de Velde, T.Petrova, RPV steel embrittlement: Damage modeling and micromechanics in an engineering perspective, Report SCK-CEN, Mol,1993
6. A.Fabry, E. van Walle, A.Verstrepen, J.Puzzolante, Th. Van Ransbeek, E.Biemiller, R. Carter, T.Petrova, Research to understanding the embrittlement behavoir of Yankee/BR3 surveillance plate and other outlier RPV steels, in Effect of Radiation on Materials, ASTM STP1270, ed. D.Gelles, R.Nanstad, A.Kumar, 1995
7. Planman T., H.Keinanen, R. Rintamaa, R.Ahlstrand, A.Kryukov, V.Nikolaev, Yu.Dragunov, Integrity assessment of the VVER 1000 RPVs, including embrittlement aspects, 5th. Int.Conf. on Material issues in design, manufacturing and operation of NPP structure component, St. Petersburg,Russia, June 19-26,1998, pp. 306-317.
8. A.Amaev, D.Erak, A.Kryukov, Radiation embrittlement of WWER-1000 pressure vessel materials, Specialist meeting on Irradiation embrittlement and mitigation, 26-29 April 1999, Madrid, Spain
9. A.Kryukov, Yu.Nikolaev, Behavior of mechanical properties of Ni alloyd RPV steel under irradiation and post irradiation annealing, Nucl.Eng.&Des., v.186(3),1998, p.353-359
10. Kryukov A.M., Yu.N.Nikolaev, T.Palnman, P.A.Platonov, Basic results of Russian WWER1000 surveillance program, Nucl. Engin. &Des. 173,1997, 333-339.

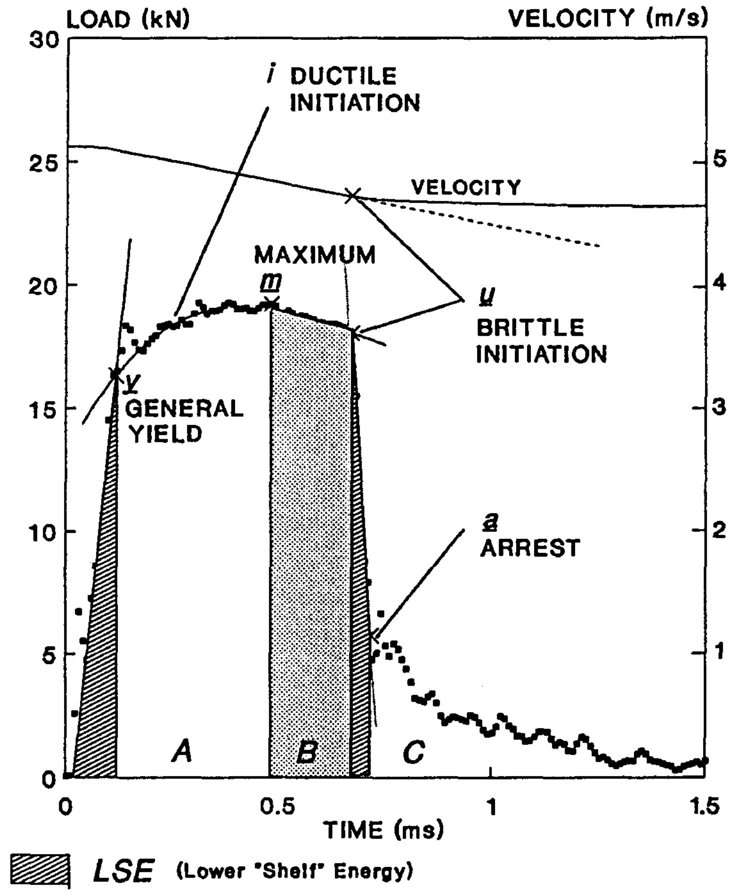
LOAD (kN)
VELOCITY (m/s)
30
25
20
15
10
5
0
5
4
3
2
1
i DUCTILE INITIATION
VELOCITY
MAXIMUM
m
u
BRITTLE INITIATION
y
GENERAL YIELD
a
ARREST
A
B
C
0
0.5
1
1.5
TIME (ms)
LSE (Lower "Shelf" Energy)

Fig.1a

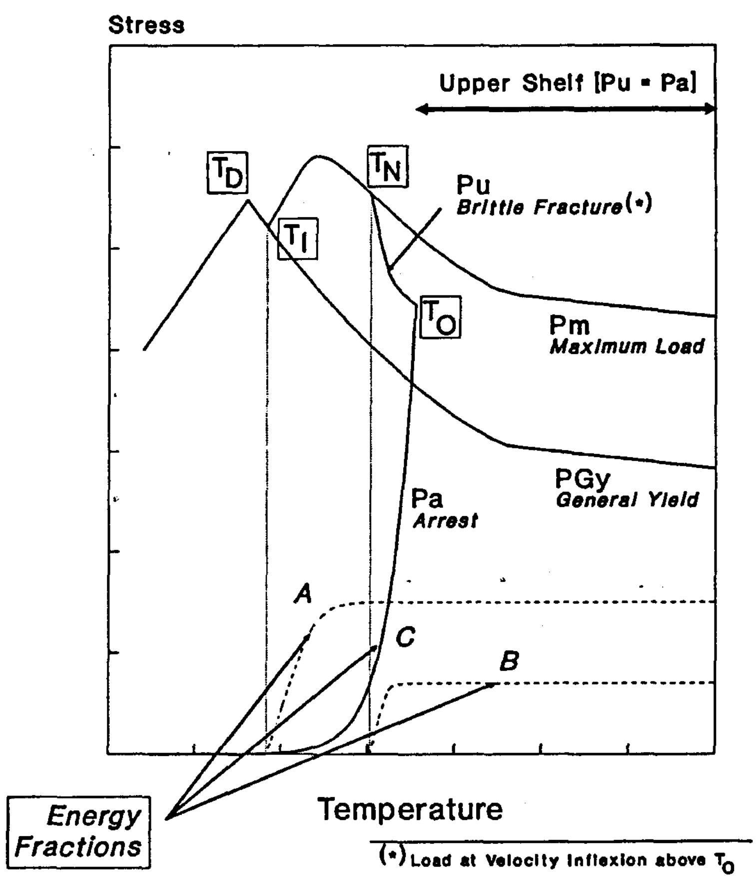
Stress
Upper Shelf [Pu = Pa]
TD
TN
TI
TO
Pu
Brittle Fracture(*)
Pm
Maximum Load
PGy
General Yield
Pa
Arrest
A
C
B
Energy Fractions
Temperature
(*) Load at Velocity Inflexion above TO

Fig.1b

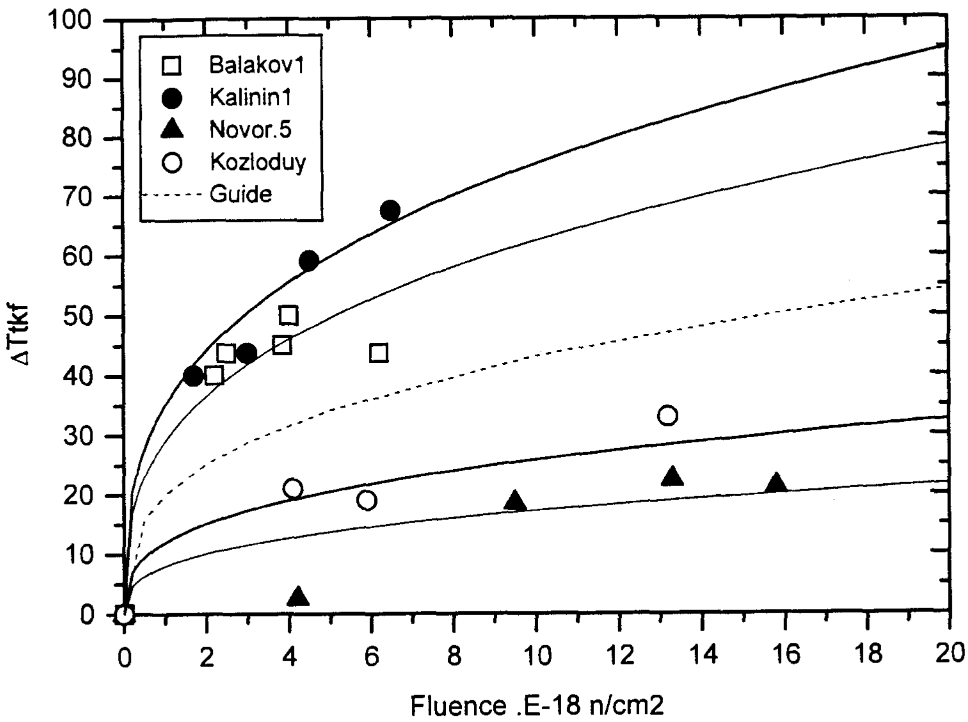
Balakov1
Kalinin1
Novor.5
Kozloduy
Guide
ΔTtkf
Fluence .E-18 n/cm2
0
10
20
30
40
50
60
70
80
90
100
0
2
4
6
8
10
12
14
16
18
20

Fig.2

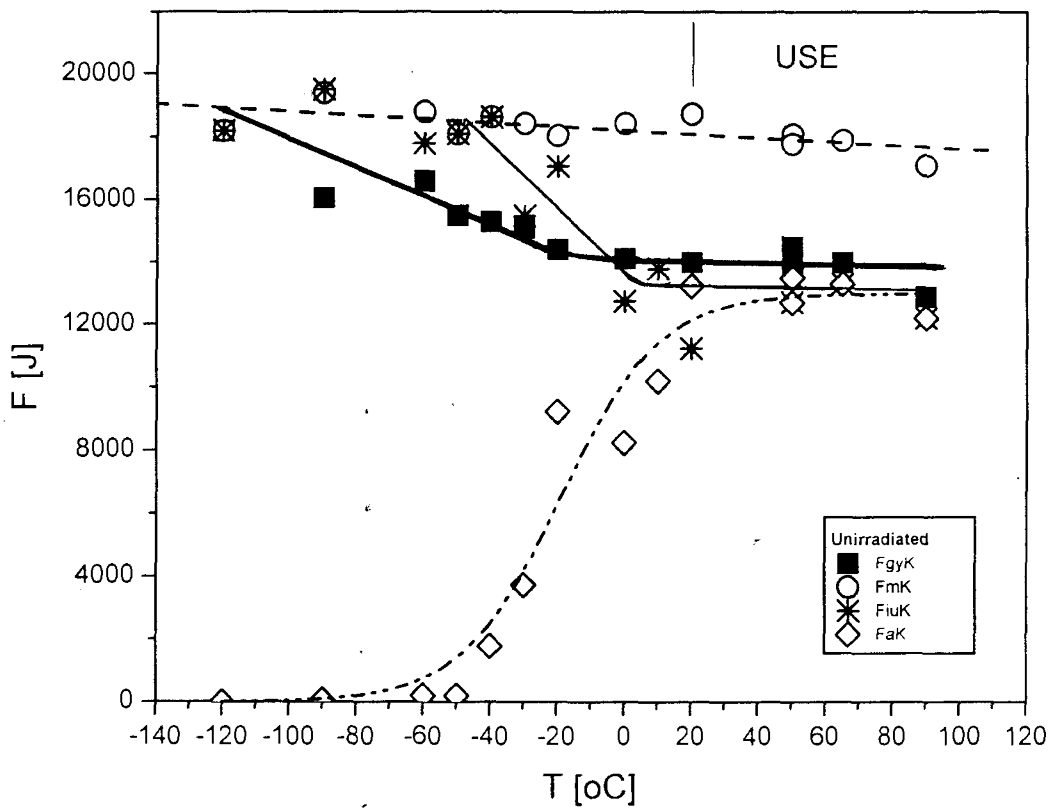
USE
Unirradiated
FgyK
FmK
FiuK
FaK
F [J]
T [oC]
0
4000
8000
12000
16000
20000
-140
-120
-100
-80
-60
-40
-20
0
20
40
60
80
100
120

Fig.3

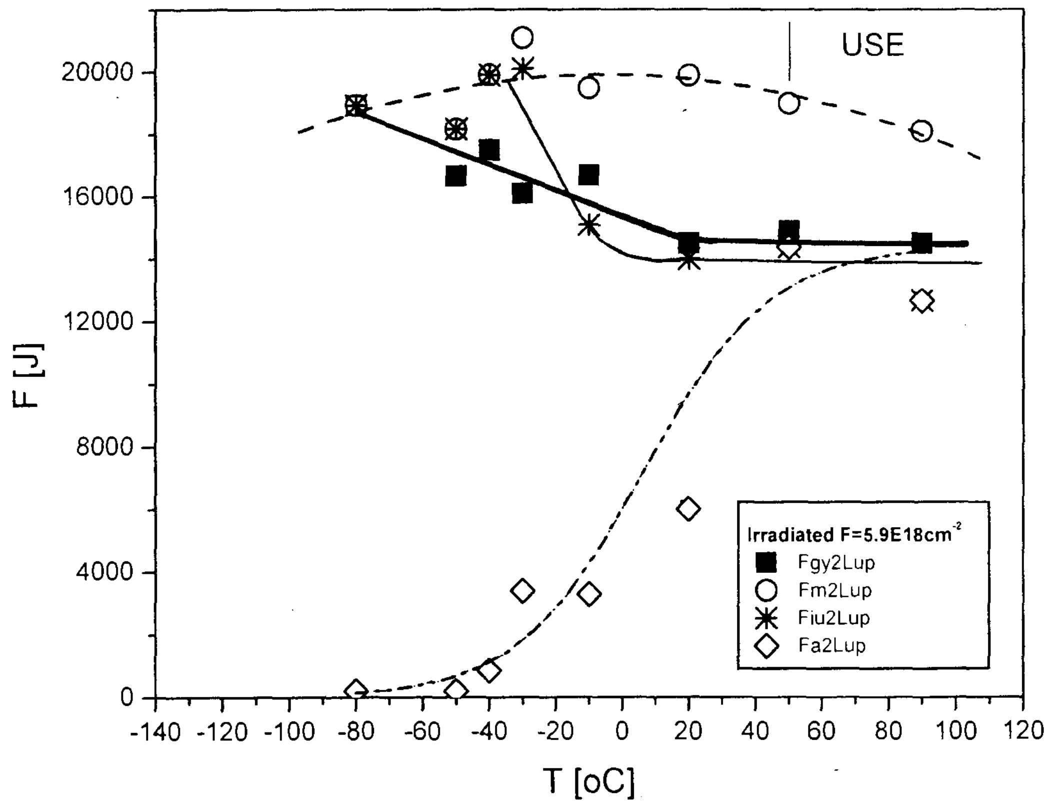
USE
20000
16000
12000
8000
4000
0
F [J]
-140 -120 -100 -80 -60 -40 -20 0 20 40 60 80 100 120
T [oC]
Irradiated F=5.9E18cm-2
Fgy2Lup
Fm2Lup
Fiu2Lup
Fa2Lup

Fig.4

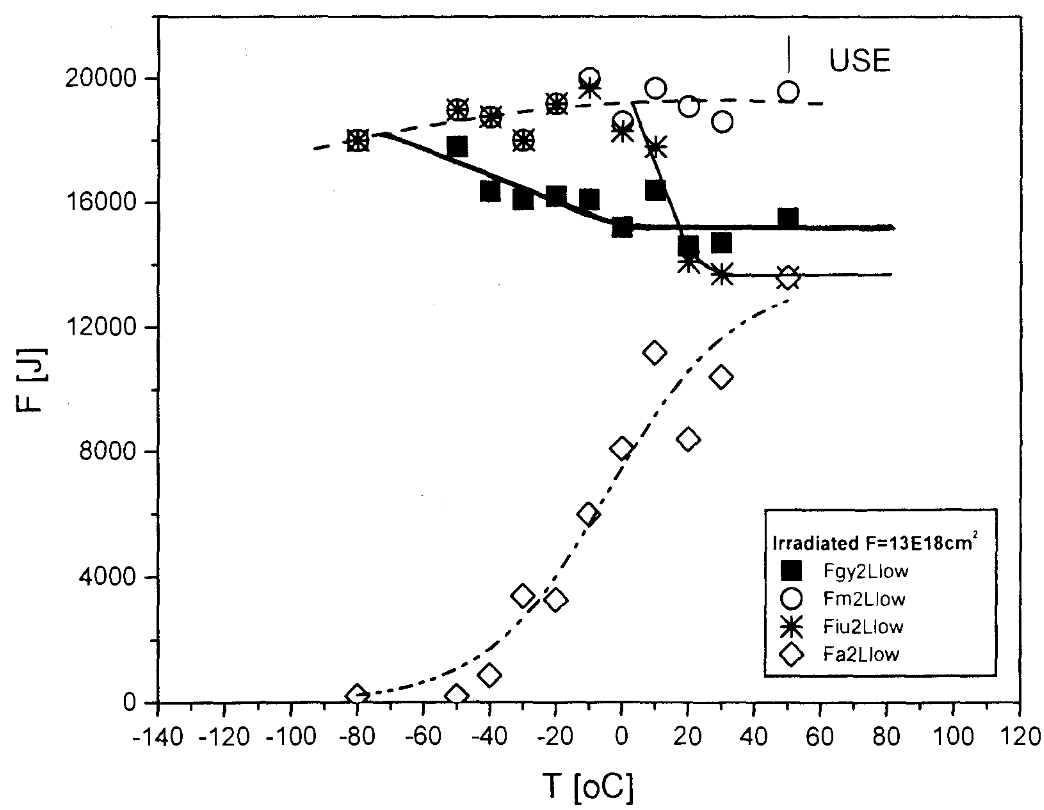
USE
20000
16000
12000
8000
4000
0
F [J]
-140 -120 -100 -80 -60 -40 -20 0 20 40 60 80 100 120
T [oC]
Irradiated F=13E18cm2
Fgy2Llow
Fm2Llow
Fiu2Llow
Fa2Llow

Fig.5

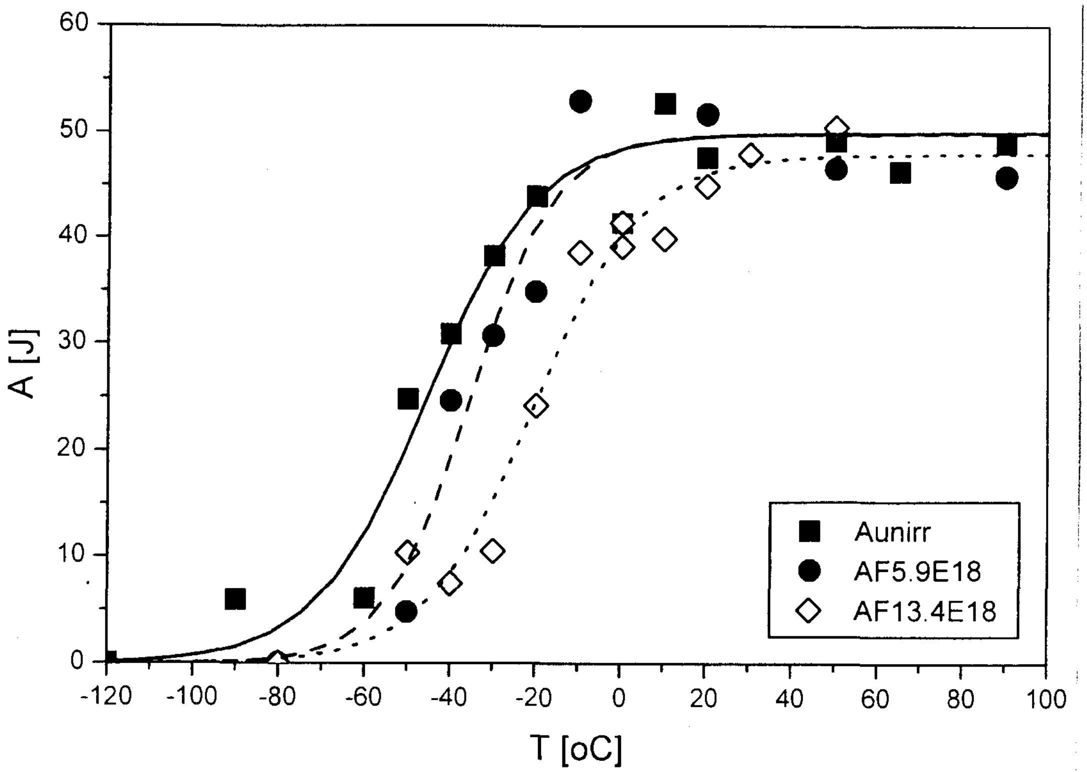

A [J]
T [oC]
Aunirr
AF5.9E18
AF13.4E18

Fig.6

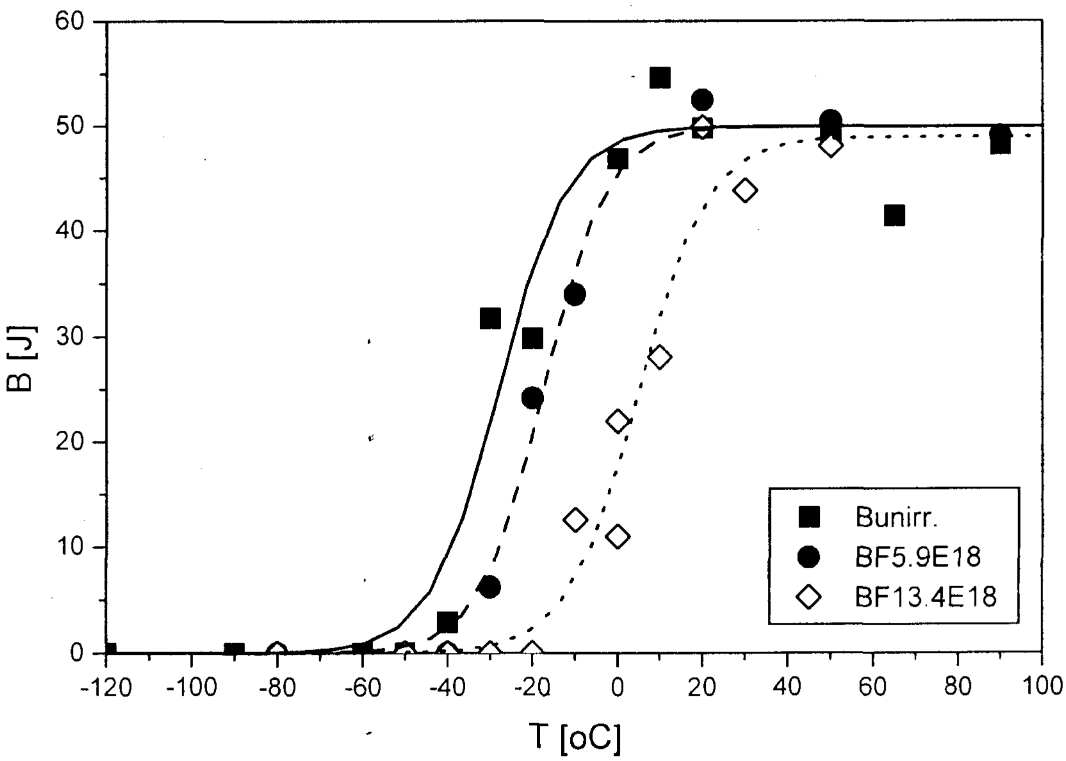

B [J]
T [oC]
Bunirr.
BF5.9E18
BF13.4E18

Fig.7

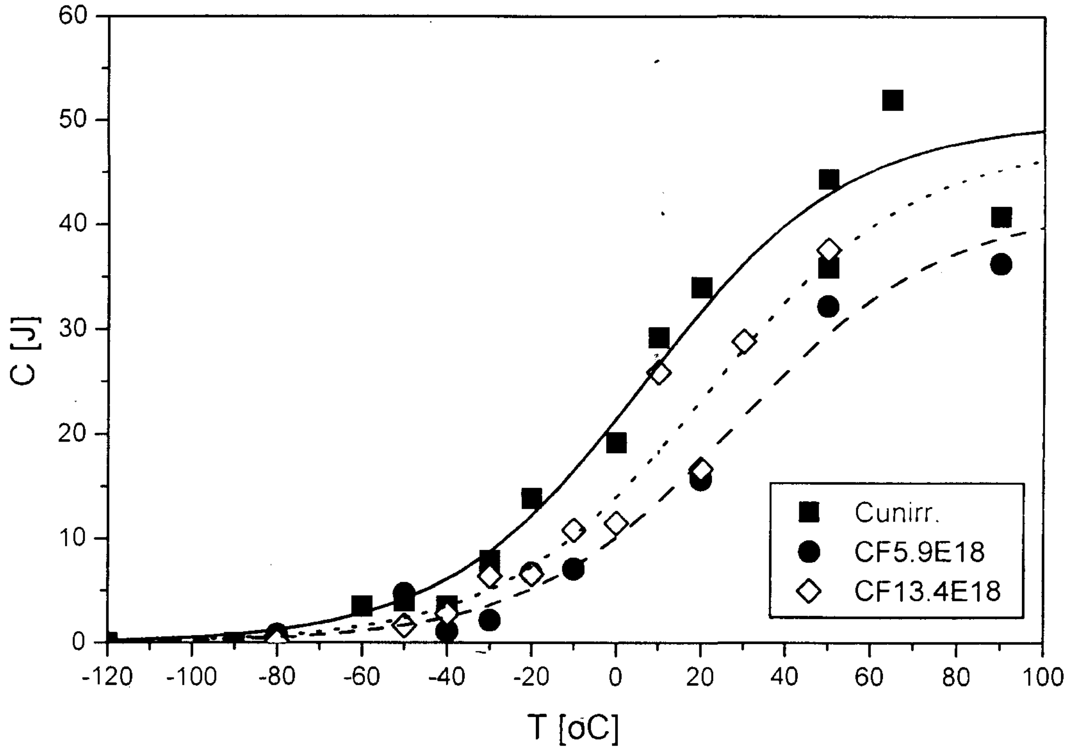

60
50
40
30
20
10
0
C [J]
-120
-100
-80
-60
-40
-20
0
20
40
60
80
100
T [oC]
Cunirr.
CF5.9E18
CF13.4E18

Fig.8